

Frascati, March 3, 2000

Note: **L-30****COUPLING IN DAΦNE**

*C. Biscari, G. Benedetti, S. Di Mitri, C. Milardi, S. Guiducci,
M.A. Preger, C. Vaccarezza, G. Vignola*

Introduction

DAΦNE *day-one* single bunch luminosity exceeded $10^{30} \text{ cm}^{-2} \text{ sec}^{-1}$. After KLOE installation single bunch luminosity never exceeded $2\div 3 \cdot 10^{29} \text{ cm}^{-2} \text{ sec}^{-1}$. A non-perfect coupling correction can be responsible for this luminosity saturation.

In the following we analyze the effect of some coupling errors at IP1.

General definitions

Let us remind some definitions concerning the coupling matrix analysis¹.

The 4x4 one-turn transport matrix **T** is written in the normal mode form as:

$$\mathbf{T} = \begin{pmatrix} \mathbf{M} & \mathbf{m} \\ \mathbf{n} & \mathbf{N} \end{pmatrix} = \mathbf{V}\mathbf{U}\mathbf{V}^{-1} \quad (1)$$

Where $\mathbf{m} = \mathbf{n} = \mathbf{0}$ for a fully decoupled point in the machine. The matrix **U** is the normal modes one-turn transport matrix:

$$\mathbf{U} = \begin{pmatrix} \mathbf{A} & \mathbf{0} \\ \mathbf{0} & \mathbf{B} \end{pmatrix} \quad (2)$$

With **A** and **B** the one-turn matrices for the two normal-modes and

$$\mathbf{V} = \begin{pmatrix} \boldsymbol{\gamma} & \mathbf{C} \\ -\mathbf{C}^+ & \boldsymbol{\gamma} \end{pmatrix} \quad (3)$$

With + denoting the symplectic conjugate. $\boldsymbol{\gamma}$ is a function of s along the ring:

$$\boldsymbol{\gamma}^2 + \|\mathbf{C}\| = 1 \quad (4)$$

$$\mathbf{V}^{-1} = \begin{pmatrix} \boldsymbol{\gamma} & -\mathbf{C} \\ \mathbf{C}^+ & \boldsymbol{\gamma} \end{pmatrix} \quad (5)$$

$$\mathbf{C}^+ = \begin{pmatrix} C_{22} & -C_{12} \\ -C_{21} & C_{11} \end{pmatrix} \quad (6)$$

This is the matrix that in MAD is denoted as R matrix in the output of the command TWISS when the COUPLE option is specified:

$$\gamma = \sqrt{\frac{1}{2} + \frac{1}{2} \sqrt{\frac{(Tr[\mathbf{M} - \mathbf{N}])^2}{(Tr[M - N])^2 + 4\|\mathbf{H}\|}}} \quad (7)$$

$$\mathbf{H} \equiv \mathbf{m} + \mathbf{n}^+ \quad (8)$$

$$\mathbf{C} = \frac{-\mathbf{H} \text{sgn}(Tr[\mathbf{M} - \mathbf{N}])}{\gamma \sqrt{(Tr[\mathbf{M} - \mathbf{N}])^2 + 4\|\mathbf{H}\|}} \quad (9)$$

The normal mode coordinates $\mathbf{a} = (a, a', b, b')$ are related to the laboratory frame via:

$$\mathbf{a} = \mathbf{V}^{-1} \mathbf{x} \quad (10)$$

and naturally viceversa:

$$\mathbf{x} = \mathbf{V} \mathbf{a} \quad (11)$$

The motion in the normal mode system is decoupled. The coordinates of any particle can be written as linear combinations of the eigenvectors of the normal system:

$$\begin{pmatrix} x \\ x' \\ y \\ y' \end{pmatrix} = \begin{pmatrix} \gamma & 0 & C_{11} & C_{12} \\ 0 & \gamma & C_{21} & C_{22} \\ -C_{22} & C_{12} & \gamma & 0 \\ C_{21} & -C_{11} & 0 & \gamma \end{pmatrix} \begin{pmatrix} a \\ a' \\ b \\ b' \end{pmatrix} \quad (12)$$

Tracking two particles with $a = 1$ and $b = 1$, which correspond respectively to the vectors:

$$\begin{pmatrix} \gamma \\ 0 \\ -C_{22} \\ C_{21} \end{pmatrix} \quad \text{and} \quad \begin{pmatrix} C_{11} \\ C_{21} \\ \gamma \\ 0 \end{pmatrix} \quad (13)$$

in the laboratory system, shows the motion of the two normal modes or its projection on the laboratory frame. The motion of the whole beam is the combination of these two normalized motions multiplied by the emittances ϵ_a and ϵ_b of the two normal modes.

The motion of a particle oscillating in one mode is a line in the plane (a,b) and an ellipse in the plane (x,y), except for the case in which $C_{12} = C_{21} = 0$, in which the motion is still a line also in the real space plane. This is the case for example in the presence of solenoids and no skew quadrupoles, in which the coupling reduces to a simple rotation of the transverse plane.

For small coupling the first (second) mode is pseudo horizontal (vertical). The ratio:

$$\kappa = \frac{\varepsilon_b}{\varepsilon_a} \quad (14)$$

is a characteristic of the whole ring, and is determined by the behaviour of the \mathbf{C} matrix around the whole ring, and of the vertical and horizontal dispersion function. In each point of the ring the dimensions in the real space (x,y) are given by the quadratic contribution of the two modes:

$$\sigma^2 = \sigma_a^2 + \sigma_b^2 \quad (15)$$

where:

$$\begin{aligned} \sigma_{x,a} &= \gamma \sqrt{\varepsilon_a \beta_a} \\ \sigma_{x,b} &= \sqrt{\varepsilon_b} \sqrt{\beta_b C_{11}^2 - 2\alpha_b C_{12} C_{11} + \gamma_b C_{12}^2} \\ \sigma_{y,b} &= \gamma \sqrt{\varepsilon_b \beta_b} \\ \sigma_{y,a} &= \sqrt{\varepsilon_a} \sqrt{\beta_a C_{22}^2 + 2\alpha_a C_{12} C_{22} + \gamma_a C_{12}^2} \end{aligned} \quad (16)$$

($\alpha_{a,b}$, $\beta_{a,b}$, $\gamma_{a,b}$ are the Twiss parameters of the two normal modes). We neglect here the contribution of the energy oscillation, i.e. in the hypothesis of zero dispersion.

In a flat beam ring and in the case of small coupling $\varepsilon_a \gg \varepsilon_b$; therefore the contribution of the second mode to the horizontal dimension can be neglected, while the contribution of the first mode to the horizontal dimension can be as large as or even larger than the second mode one: since the vertical dimension is modulated by β_b , for what concerns the second mode oscillation, in the low- β region the term proportional to the first mode invariant can be dominating, if the elements C_{12} and C_{22} of the coupling matrix are not zero.

Another significant parameter is the angle between the axis of the normal mode oscillations and the real space.

The angle between the principal axis of the modes and the real plane are:

$$\begin{aligned} \theta_a &= C_{22} + \frac{\alpha_a}{\beta_a} C_{12} \\ \theta_b &= C_{11} - \frac{\alpha_b}{\beta_b} C_{12} \end{aligned} \quad (17)$$

In the waist position the angle is defined only by the diagonal elements, and if $C_{11} = C_{22}$ the two modes are orthogonal.

Application to DAΦNE

Let us consider the case of DAΦNE around IP1 (KLOE). In the nominal case the coupling at the IP is fully corrected and the matrix $\mathbf{C} = \mathbf{0}$. Near the IP, in between the low- β triplets, the coupling is determined only by the KLOE solenoidal field.

The ring is described in the MAD format by the decoupled KLOE interaction region and the decoupled ring. Nominal IP parameters and tunes are considered. The emittances are computed by MAD. All the parameters and the matrix **C** at the IP are summarized in Table I.

Table I - Nominal parameters

Mode	1	2
ϵ (mm mrad)	0.8175	0.4021e -09
κ (%)	0.00	
β^* (m)	4.500	0.045
α^*	0.000	0.000
Q	5.150	5.210
	$C_{11} = 0$ $C_{21} = 0$	$C_{12} = 0$ $C_{22} = 0$

Figure 1a shows the projection in the real plane (x,y) of the first mode motion of a particle having the invariant of 1mm at the IP, followed in nine points along z (from z = -12 cm to z = 12 cm) in steps of 3 cm. Figure 1b corresponds to the second mode projection of a particle having an invariant of 0.01 mm. In the figures the vertical scale is 1/100 of the horizontal one. The projections of the two mode motions on the real plane lay in this case on two perpendicular lines and follow the rotation of the transverse plane induced by the solenoid (in this scale the diagonals of each square have an angle of $\pm 0.57^\circ$).

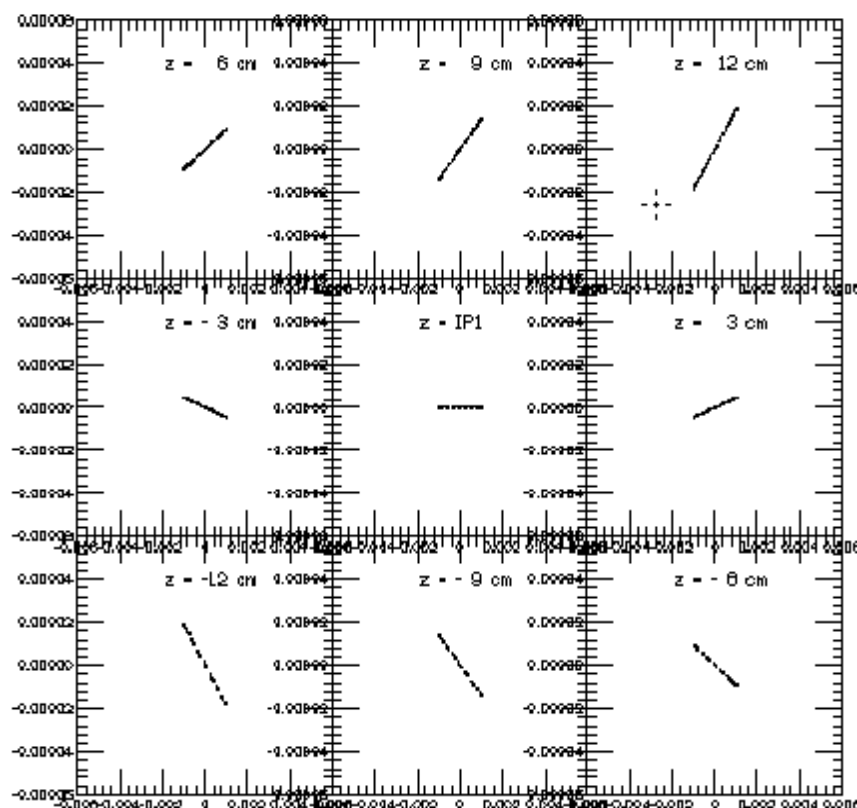


Figure 1a - Mode 1 projection in the (x,y) plane for the nominal case.

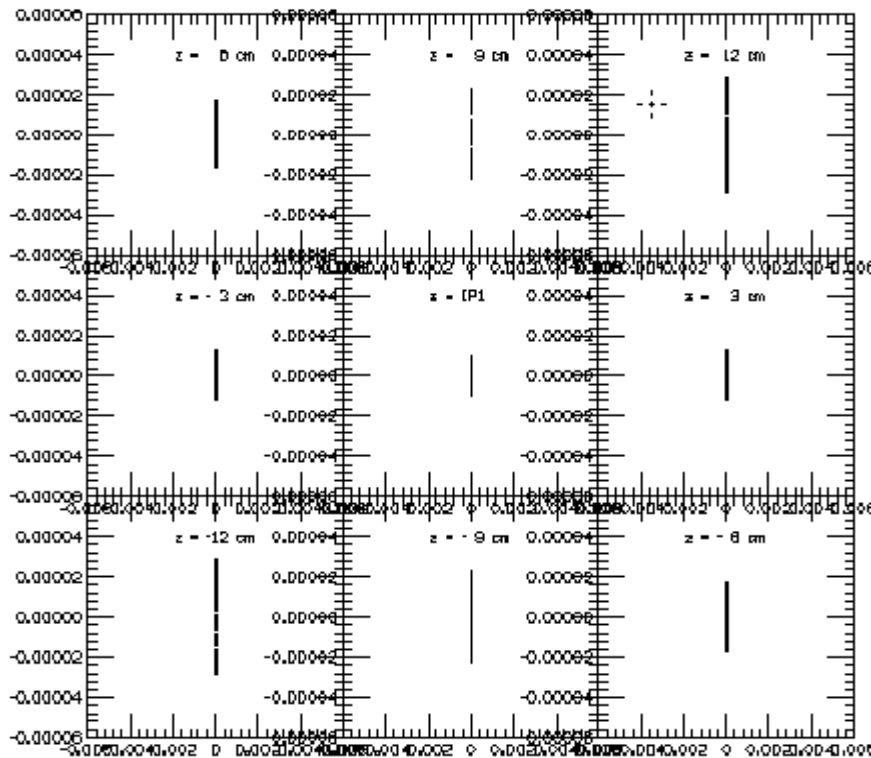


Figure 1b - Mode 2 projection in the (x,y) plane for the nominal case

The whole beam motion will be a composition of both modes. Figure 2 shows the projection for the nominal case of the ellipse defined in the normal mode plane by the curve:

$$\frac{a^2}{\sigma_a^2} + \frac{b^2}{\sigma_b^2} = 1 \quad (18)$$

with

$$\sigma_a = 1 \text{ mm} \quad (19)$$

and

$$\sigma_b = \frac{\sigma_a}{100} \quad (20)$$

which corresponds to the nominal emittance ratio $\kappa = 0.01$.

At the IP of course the projection is a circle, while around the IP it is an ellipse with axis modulated by the betatron functions β_a, β_b . To be noticed that the invariant emittance in the second mode plane is not induced by any coupling in the ring, since $\kappa = 0$ as specified in table I.

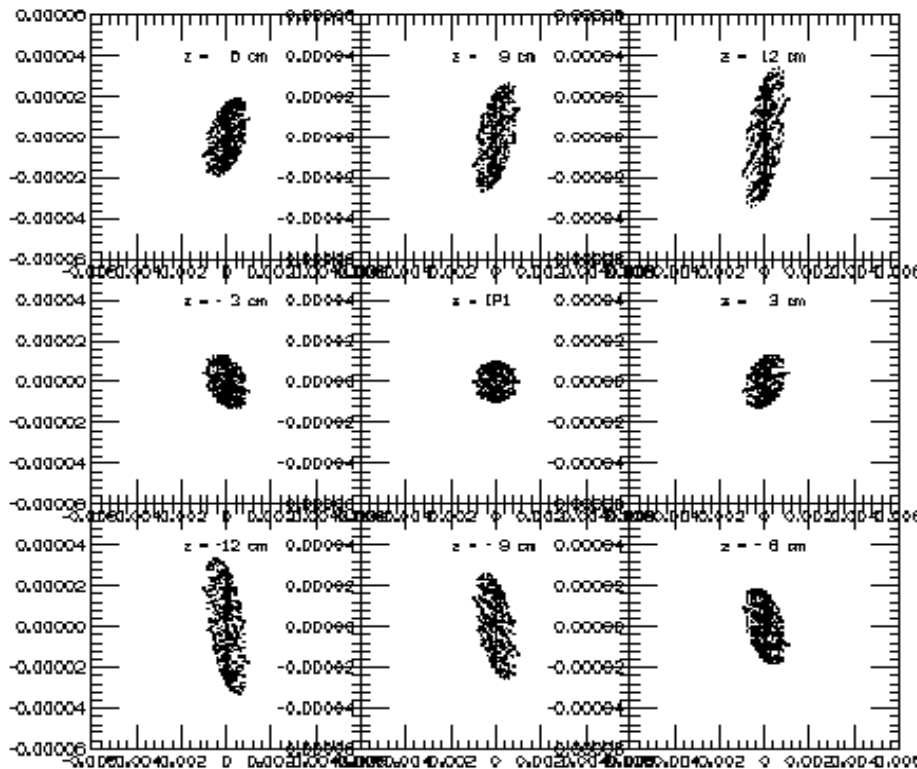


Figure 2 - Projection in the (x,y) plane of the nominal ellipse for the nominal case

Let us consider now the case of a machine with a coupling source, for example in the case of a solenoidal perturbation, as an asymmetry of the solenoidal compensation in DAΦNE which introduces a value of $\kappa \approx 0.01$. We have considered the case in which one of the compensator field integral is increased by 9%, giving a change in the tunes and a slight mismatch of the betatron function at the IP1 (see Table II). Figures 3a and 3b represent the two normal modes projections in the (x,y) plane. The projection of the first mode is not anymore a line, but an ellipse, with variable modulation. Furthermore the tilt angle is not zero at the IP. The composition of the two modes (see Fig. 4) shows that the motion is dominated by the first mode. The maximum density is still at the IP, while the maximum vertical oscillation is a factor two above the nominal one.

Table II - Asymmetric error in the compensation

Mode	1	2
ϵ (mm mrad)	0.7806	0.7835E-02
κ (%)	1.00	
β^* (m)	4.191	0.047
α^*	-0.046	-0.041
Q	5.161	5.219
	$C_{11} = -1.083$ $C_{21} = -0.074$	$C_{12} = -0.001$ $C_{22} = -0.013$

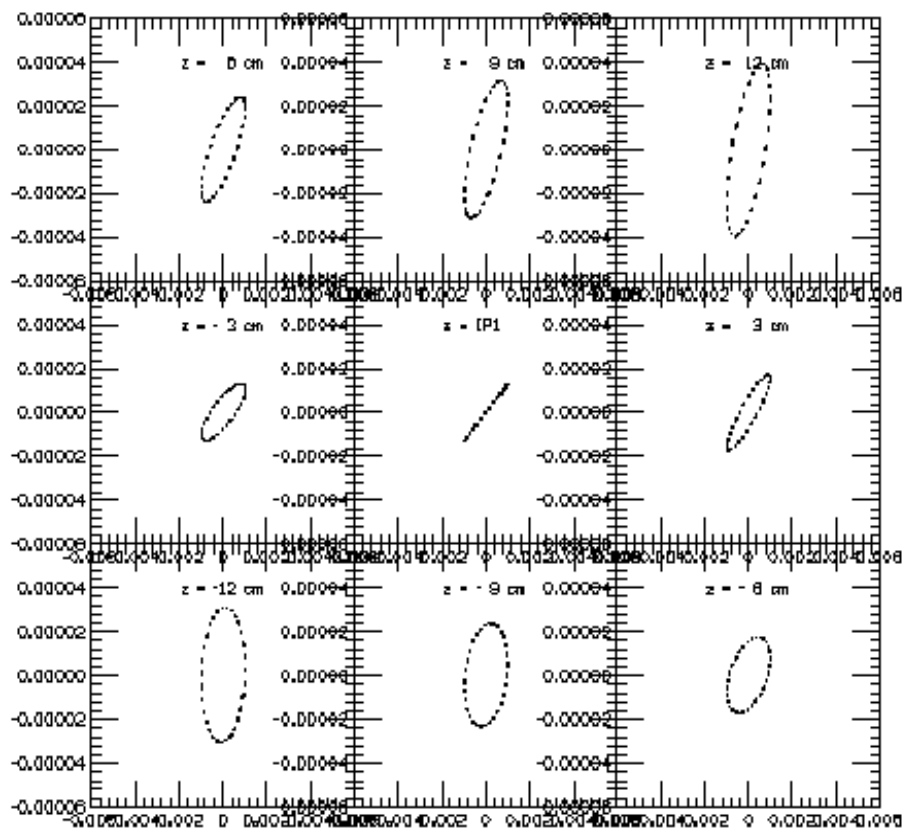


Figure 3a - Mode 1 projection in the (x,y) plane for asymmetric compensators

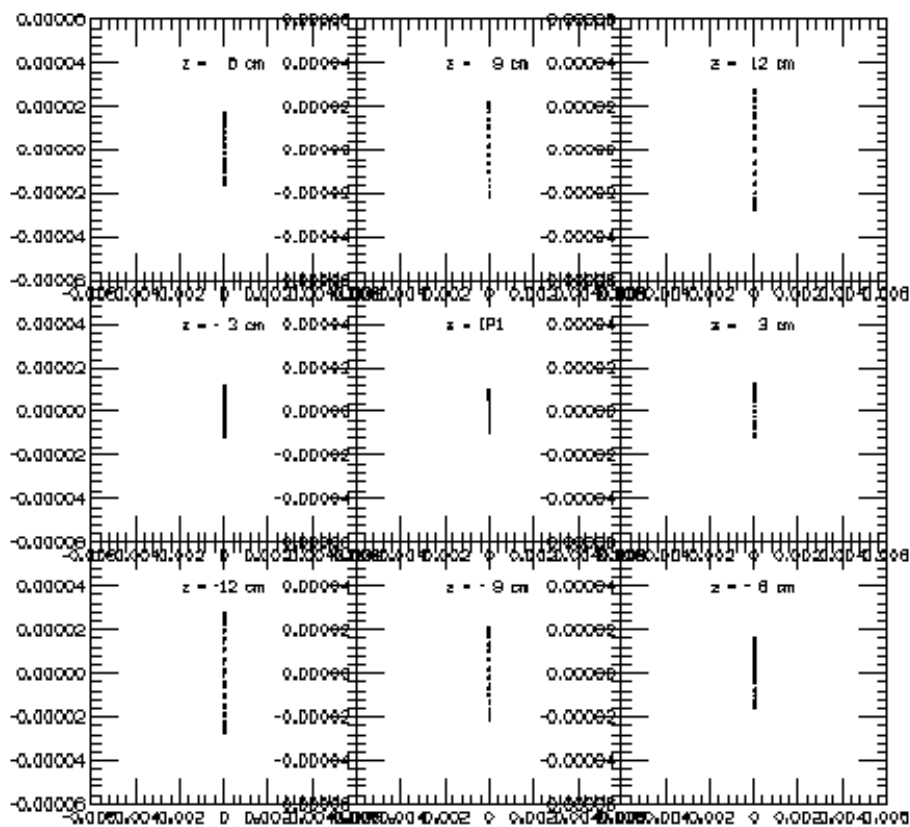


Figure 3b - Mode 2 projection in the (x,y) plane for asymmetric compensators

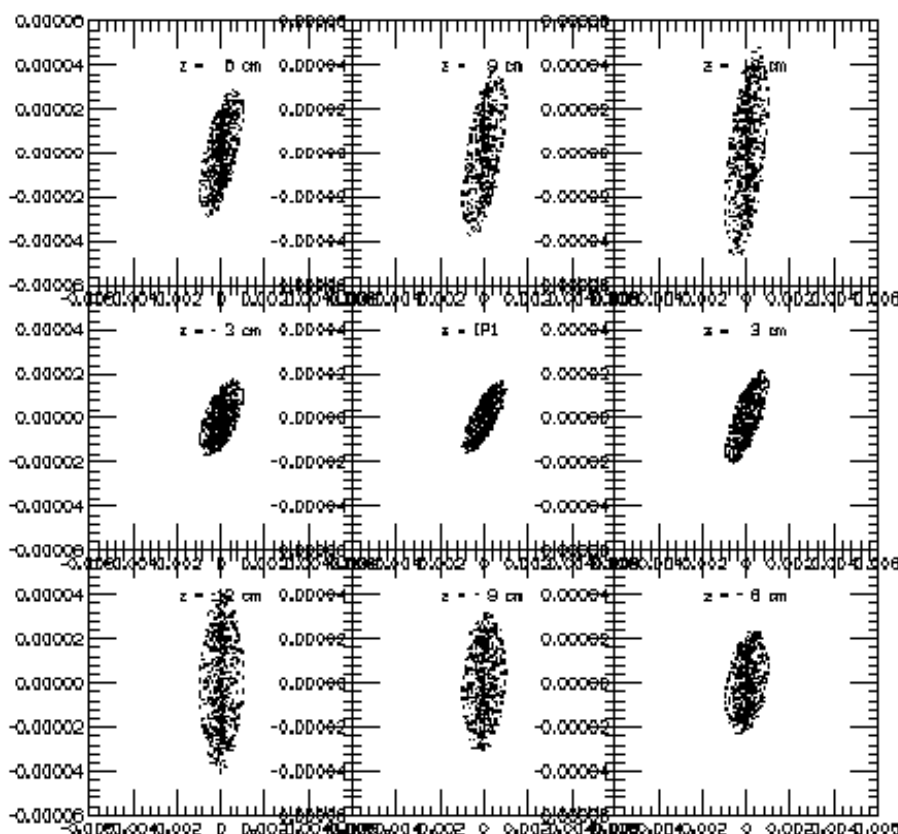


Figure 4 - Projection in the (x,y) plane of the transverse ellipse for asymmetric compensators

Effects of different source of coupling at the IP

Let us consider the nominal optics: low- β at the IP ($\alpha_x = \alpha_y = 0$) and decoupled one-turn transport matrix ($\mathbf{C} = \mathbf{0}$).

Symmetric perturbation

Any source of coupling symmetric around the IP will in this case produce a variation in κ , but no tilt of the transverse plane at the IP: $C_{11} = C_{22} = 0$. This is true for both solenoidal symmetric fields or anti-symmetric skew-quadrupolar perturbation.

Figure 5 shows the example of the (x-y) plane around the IP in the case of a symmetric tilt error (0.3°) on the two nearer quadrupoles around the IP giving $\kappa = 1\%$ (see Table III). The beam size at the IP is increased with respect to the nominal case since the contribution of the first mode is of the same order of the second one; the derivative of the tilt angle has the opposite sign with respect to the nominal one (see Fig. 2).

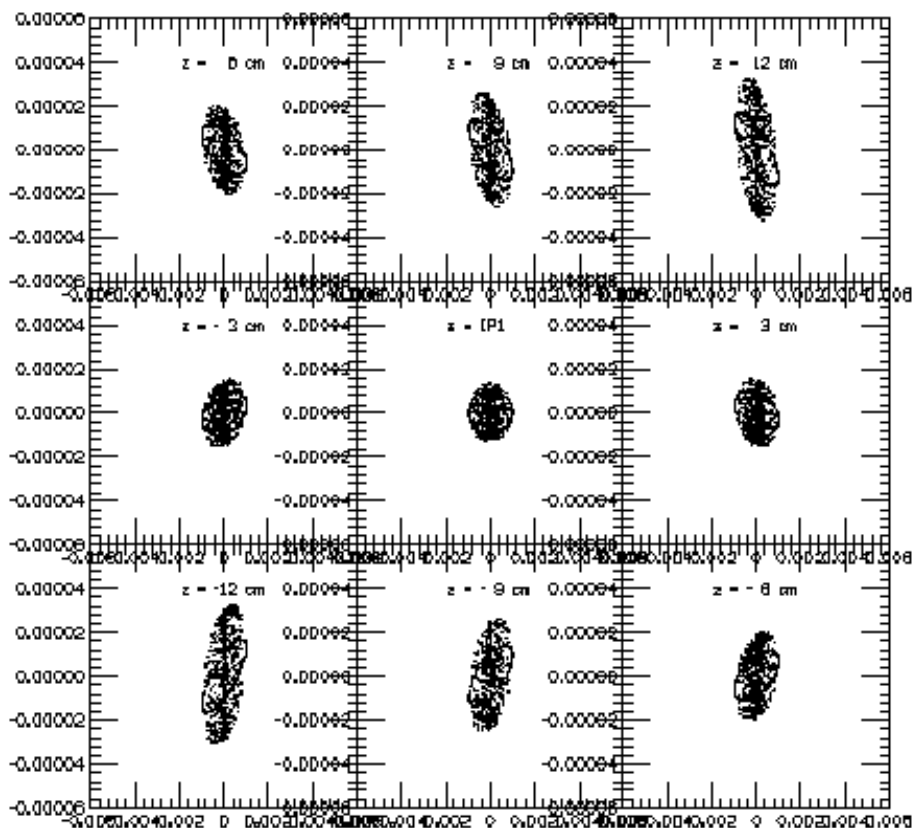


Figure 5 - Projection of the transverse ellipse in the (x,y) plane for antisymmetric skew perturbation

Table III - Antisymmetric skew perturbation

Mode	1	2
ε (mm mrad)	0.8046	0.7789E-02
κ (%)	0.97	
β^* (m)	4.521	0.045
α^*	0.000	0.000
Q	5.149	5.211
	$C_{11} = 0$ $C_{21} = -0.264$	$C_{12} = 0.043$ $C_{22} = 0$

No tilt at the waist position will be induced by the KLOE IR optics if the two compensators are symmetrically powered, if the two triplets are tilted by the same angle, even if not the one giving the better κ , if the field integral of the KLOE detector is symmetric around the IP. Any of these effects will on the contrary produce changes in the tilt derivative around the IP.

Asymmetric perturbation inside the IR

Any asymmetry inside the IR will produce a tilt at the IP.

What is then the relative angle between the two beams? Let us assume that the nominal rings have the same one-turn transport matrix at the IP, thus meaning they have same tunes, same betatron functions $\beta_{1,2}^*$ and $\alpha_x = \alpha_x = 0$.

Any perturbation which is in the common part around the IP will produce the same tilt on both rings, so that the relative tilt will be zero, as long as the above conditions are satisfied.

A perturbation coming from any other point of the rings will act in a different way on the two beams, even if it comes from the second common IR, since the phase advance from the perturbation to IP1 will be different for the two rings.

About the KLOE IR

The design parameters of KLOE IR correspond to a value of the longitudinal magnetic field at the IP of 0.6 T, achievable with a current of 2660 A up.

From the measurements of March 1999 the alignment of the two low- β triplets showed a tilt error of $+0.7^\circ$ (quads QUAKI101, 2, 3) and -1° (quads QUAKI104, 5, 6), going in both cases in the direction of lowering the nominal tilt angle. This fact led us to work with a lower field in the KLOE detector. Even if to completely cancel the tilt error the field should have been lowered by 14% (2330 A, 0.525 T), it was agreed with the KLOE group to work with a field of 0.564 T corresponding to 2500A.

The compensator fields have been empirically set to better correct the coupling at the values of 82 A, corresponding to the 82% of the nominal set, working therefore with an integral field lower than the KLOE one, as long as the calibrations of the three magnets can be trusted.

Let us now analyze the effects on the coupling of each one of the involved elements, comparing each case with the completely decoupled case, which corresponds to table I (0.525 T in KLOE, 88 A on the compensators, assumed equal, tilt errors on the triplets equal on both sides: ± 0.85 and slightly corrected values of the individual tilt of the quads).

Compensator fields

The effect of changing the field in both compensators symmetrically is shown in Fig. 6.

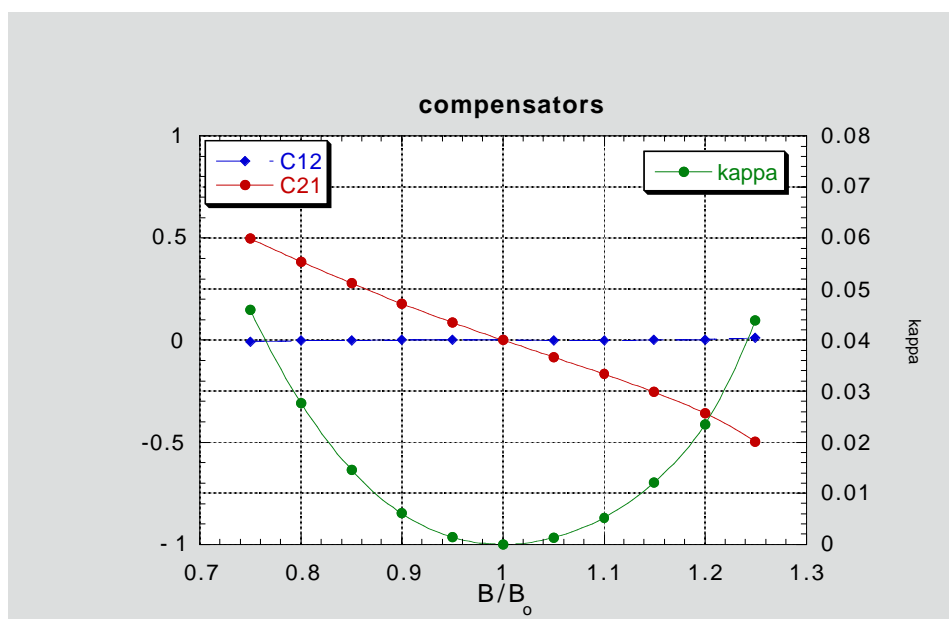


Figure 6 - Beam emittance ratio and C Matrix dependence on compensator fields.

The value of κ (kappa in the plots) remains less than 2% for changes of the order of $\sim 15,20\%$ and is reasonably symmetric for positive or negative changes. This effect has been in fact observed in DAΦNE when moving the compensator fields by a large amount and not observing big changes in the emittance value and/or in the minimum tune distance. The diagonal elements of the C matrix at the IP are zero, (tilt angle zero), C_{21} changes almost linearly while the value of C_{12} is very small, which means that the projection on the vertical plane of the first mode is negligible.

KLOE field

The KLOE field variation is felt stronger from this point of view: fig 7 shows the same functions; notice that the horizontal scale is half the one in the above figure. The asymmetries in the curves are due to the presence of the quadrupoles inside the field. The value of $\kappa = 2\%$ is reached with field variations of -5% , $+7\%$. In this case the element C_{12} is not zero, which gives a contribution in the vertical dimension.

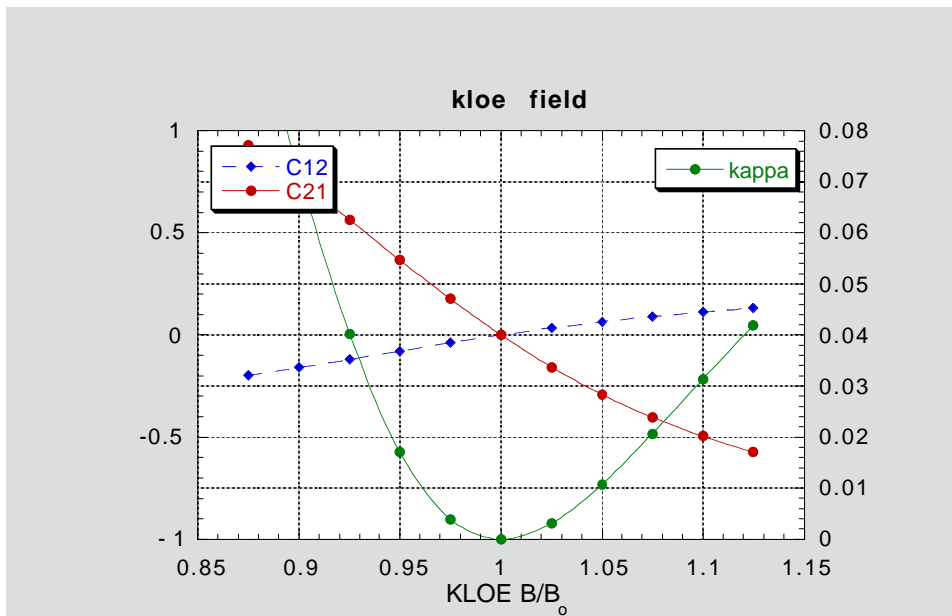


Figure 7 - Beam emittance ratio and C Matrix dependence on KLOE field

Present working point

Let us see now which is the present situation: Figure 8 corresponds to the variation of the compensators around the present value and the present KLOE field. The emittance of the second mode can be even zeroed lowering the compensator field to about 70A. This unfortunately does not eliminate the vertical component of the motion, since $C_{12} \sim 0.08$ and therefore

$$\sigma_y = \sqrt{\varepsilon_a} \sqrt{\frac{C_{12}^2}{\beta_a}} \approx \sqrt{0.0014\varepsilon_a} \approx 1.8\sigma_{ynom} \tag{21}$$

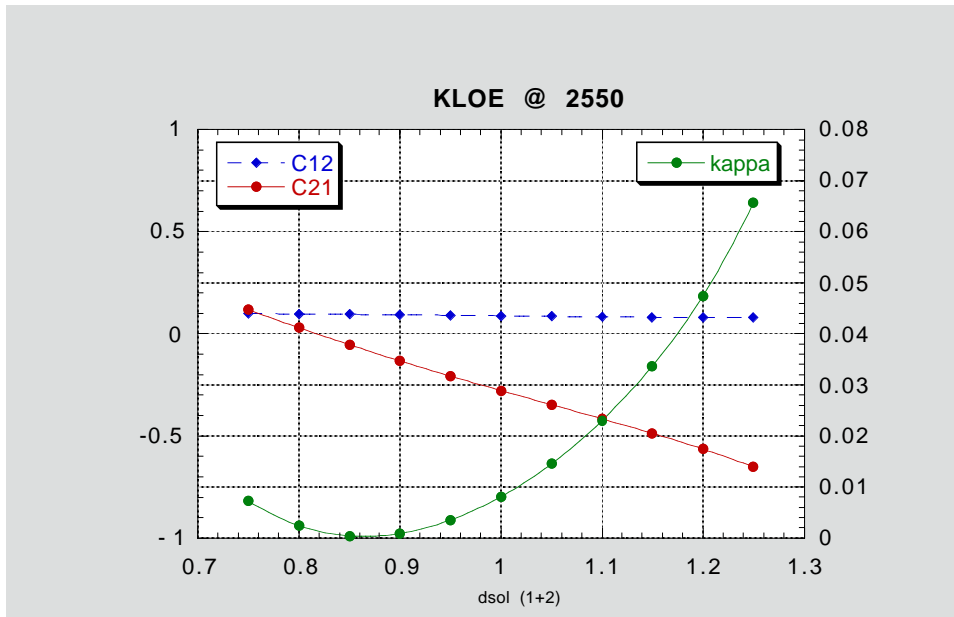


Figure 8 - Beam emittance ratio and C Matrix dependence on compensator fields for present value of KLOE field

With the present KLOE field and taking into account the measured tilt angles of the quads, it can be computed a correction to decouple the machine at the IP, using the skew quads in the short and long arc around KLOE, and keeping low the value of κ ; with this arrangement the vertical dimension at the IP is determined only by the mode 2 emittance, since the first mode is purely horizontal.

With the four skew quadrupoles powered as:

QSKEL106	63.4 A
QSKEL103	-2.8 A
QSKES104	13.0 A
QSKES101	2.5 A

and the compensators lowered by 12% (73 A) the computed emittances are $\epsilon_a = 0.86$ mm mrad and $\epsilon_b = 0.30E-02$, corresponding to $\kappa = 0.3\%$.

This means that the residual emittance coupling due to the mismatch between the present KLOE field and the tilt angle of the low- β triplets, if properly corrected, can be smaller than the nominal design value.

References

- [1] D. Sagan and D. Rubin, Linear analysis of coupled lattices, Physical Review Special Topics- Accelerators and Beams, Volume 2, 074001 (1999).